JMEPEG (2011) 20:1569–1574
DOI: 10.1007/s11665-011-9843-1

1059-9495/$19.00

Tensile Behavior of Ultrafine-Grained Al-4Zn-2Mg Alloy Produced by Cryorolling

K. Gopala Krishna, Nidhi Singh, K. Venkateswarlu, and K.C. Hari Kumar

(Submitted October 19, 2010; in revised form December 15, 2010)

An Al-4Zn-2Mg alloy was subjected to cryorolling (CR) followed by short annealing. An average grain size of ~100 nm was achieved. Cryorolled samples showed large reduction in grain size due to suppression of dynamic recovery and absence of annihilation of dislocations, as compared to room temperature rolled samples. Further, the ultrafine-grained (UFG) Al-4Zn-2Mg alloy when subjected to natural aging showed an improved strength of ~413 MPa with ductility of ~25%, as compared to ~360 MPa and 22% ductility in peak aged condition of coarse-grained alloy. However, UFG alloy in peak aging condition, exhibited a relatively strength (~375 MPa) and 24% ductility combinations than the natural aging condition. The latter is attributed to dynamic precipitation and stored energy. In the present study, it is demonstrated that simultaneous improvement in strength as well as ductility can be achieved for the Al-4Zn-2Mg alloy through CR and controlled heat treatment combinations.

Keywords aging, Al-4Zn-2Mg alloy, cryorolling, secondary precipitation, tensile behavior, ultrafine-grain structure

1. Introduction

Aluminum and its alloys are extensively used for various design engineering applications, where the high strength to weight ratio is one of the basic criteria. In the recent past, ultrafine-grain (UFG) and nano-crystalline materials obtained by severe plastic deformation (SPD) have attained significant importance due to their superior mechanical properties. Formation of UFG structure in materials is a technologically interesting phenomenon as it enables an increase in strength without any significant degradation in toughness, elastic moduli, diffusivity of solute, etc. (Ref 1-3). Refinement of the microstructure can be achieved through SPD techniques, which include high-pressure torsion, reciprocal extrusion, equal-channel angular pressing (ECAP) (Ref 4-6), accumulative roll bonding (Ref 7-10), repetitive corrugation and straightening (Ref 11-13), constrained groove pressing (CGP) (Ref 14), and constrained groove rolling (CGR) (Ref 15), etc. These processes generally result in materials with UFG (<1 μm) structure. Though such materials exhibit higher strength, they lack good ductility. Several efforts have been made in the past to achieve both, high strength and good ductility, simultaneously.

Cryorolling (CR) was proved to be an effective method for enhancing both tensile strength and yield strength of the AA5083 Al alloy (Ref 16). About 10% increase in yield strength was reported for cryorolled AA5083 Al alloy, as compared to the same alloy, rolled at room temperature with the same reduction ratio. Suppression of dynamic recovery during deformation at cryogenic temperature was found to be the reason (Ref 4) for enhanced strength due to high density of defects generated by deformation, which act as potent recrystallization sites. It is also reported that rolling of commercial purity Cu at cryogenic temperature, resulted in UFG structure at lower plastic deformation when compared to other SPD processes, at ambient or elevated temperatures (Ref 5).

One of the successful methods for increasing the strength while retaining the ductility, with respect to heat treatable Al alloys, was CR involving several steps of processing (Ref 6), i.e., (1) solutionizing the alloy to dissolve all second-phase particles and then quenching to produce a supersaturated solid solution; (2) CR at liquid nitrogen temperature to produce heavily deformed structure; (3) short annealing to produce UFG microstructure; and (4) aging to produce homogeneously distributed strengthening precipitates. An AA 2219 Al alloy, that was subjected to CR and subsequent annealing and aging, was reported to have a grain size in the range of 500 nm to 1 μm with UTS of 540 MPa and while retaining the ductility at 11% (Ref 17).

Both high strength and high ductility in a AA 2024 Aluminum alloy was obtained by CR with an approach involving (i) solution treatment, (ii) CR to produce a fine-grain structure with high density of dislocations, and (iii) aging to generate highly dispersed nano-sized precipitates (Ref 18). The objective of the present work was to obtain UFG structure in an Al-4Zn-2Mg alloy using CR technique followed by short annealing and to study its tensile behavior after aging. This alloy is currently used in automobile and aerospace industries and other structural applications.

K. Gopala Krishna, National Metallurgical Laboratory (CSIR), Madras Centre, Chennai 600113, India; **Nidhi Singh**, National Physical Laboratory (CSIR), New Delhi 110012, India; **K. Venkateswarlu**, National Aerospace Laboratory (CSIR), Bangalore 560017, India; and **K.C. Hari Kumar**, Department of Metallurgical and Materials Engineering, Indian Institute of Technology, Madras, Chennai 600036, India. Contact e-mail: karodi2002@yahoo.co.in.

2. Experimental Material and Procedure

Al-4Zn-2Mg alloy in the form of plates of thickness 6 ± 0.08 mm in T6 temper (peak aged in two steps, at 100 °C for 5 h and 150 °C for 6 h) were selected as starting materials. The chemical composition of the alloy is shown in Table 1. A 25×100 mm size strips were cut from the plates and solutionized at 480 °C for 1 h, followed by water quenching. The solutionized strips were subjected to CR as well as room temperature rolling (RR). CR was carried out by dipping the strips into liquid nitrogen for ~10 min before first pass and 2 min for each subsequent pass, during rolling. The temperature of the plate during CR was about ~−170 °C. Such specimens from both CR and RR were chosen, which had comparable hardness after rolling, even though their deformation levels were different. Both CR (80% reduction) and RR (85% reduction) strips were subjected to short annealing treatment for 3 min at 150 ± 2 °C to facilitate recovery and partial recrystallization leading to the formation of UFG structure. Short annealed strips were given both natural aging (CRNA, RRNA) and artificial peak aging (CRPA, RRPA) treatments as specified in Table 2.

Hardness was measured using the Indentec® Vickers hardness with a load of 5 kg. Miniature-sized flat tensile specimens; with 5 mm gage length and thickness of ~1 mm were prepared from the strips, along the rolling direction. Tensile tests were carried out at a nominal strain rate of 3×10^{-3}/s on an Instron machine of 10 kN capacities. All the tensile tests were carried out at ambient temperature. Microstructural characterization was carried out using Leica Optical and Philips CM-12 transmission electron microscope (TEM). For metallographic examination, samples were prepared by electrolytic etching, using Barker's reagent (4-5 mL fluoroboric acid in 200 mL water) on mirror polished samples. For TEM study, thin discs were sliced from the strips using slow speed cutter which were mechanically thinned down to 100 µm. These 3 mm discs were further thinned down using twin-jet electropolishing technique at 15 V in a mixture of 30% nitric acid and 70% methanol maintained at ~20 °C.

Table 1 Chemical composition of the alloy

Zn	Mg	Mn	Si	Fe	Zr	Al
4.09	1.03	0.3	0.16	0.33	0.18	Bal.

3. Results and Discussion

The optical image of the Al-4Zn-2Mg alloy in coarse-grain peak aged (CGPA) condition is shown in Fig. 1(a). The average grain size is 80 ± 13 µm, obtained by linear intercept method, employing the image analysis system with optical microscope. Both Mg_2Si and Fe-rich intermetallics can be clearly seen in Fig. 1(a). To identify these particles, they were chemically extracted from the alloy and their SEM image is shown in Fig. 1(b). XRD results clearly demonstrate the presence of Mg_2Si and Fe-rich intermetallics (Fig. 1c). SEM EDAX results also confirmed the presence of these particles and a representative EDAX taken on Mg_2Si particle is shown in Fig. 1(d). From TEM images, it is revealed that both stable (η) and metastable (η′) precipitates, with the size range of 1-10 nm, were uniformly distributed in the Al matrix. The optical image of cryorolled sample in which the fractured intermetallics are present along the rolling direction, is shown in Fig. 2(a). TEM image of coarse precipitates of $MgZn_2$ along the grain boundaries with associated precipitate free zones (PFZ) is shown as an inset in Fig. 2(b).

The hardness of the solutionized and water quenched Al-4Zn-2Mg alloy after rolling is 50 HV. After deformation up to a true strain of ~1.3, the hardness is increased to ~128 HV and ~133 HV for room temperature and cryorolled conditions, respectively. The effect of true strain on the variation of hardness is shown in Fig. 3 for the CR and RR samples. When the strain is increased to ~2.4, further improvement in hardness up to 142 HV and 147 HV, have been observed for RR and CR samples, respectively. The increase in hardness is continuous as the strain is increased, and is slightly higher for CR than RR at all strains employed in the study. The rolled samples were short annealed to facilitate recovery and recrystallization and then subjected to natural aging and peak aging treatments. The corresponding mechanical properties are shown in the Table 2 and the tensile and work hardening behavior of the alloy is shown in Fig. 4(a) and (b).

The UTS values for the CRPA and CRNA, 390 and 415 MPa, respectively, are higher than the coarse-grained peak aged (CGPA) alloy. There has been ~10% improvement in the strength values, while the ductility level is also increased by

Table 2 Tensile properties of CG and UFG alloy after different aging treatments

Sample description (code)[Aging condition]	YS, MPa	UTS, MPa	Elongation[a], %
Coarse-grained peak aged (CGPA) [100 °C/5 h + 150 °C/6 h]	290	361	21.5
Cryorolled peak aged (CRPA) [100 °C/5 h + 150 °C/90 min]	320	390	23.5
Cryorolled naturally aged (CRNA) [At room temperature for 180 days]	260	413	25
Room temperature rolled, peak aged (RRPA) [100 °C/5 h + 150 °C/90 min]	297	375	11
Room temperature rolled, naturally aged (RRNA) [At room temperature for 180 days]	335	400	14

[a]Gage length = 5 mm

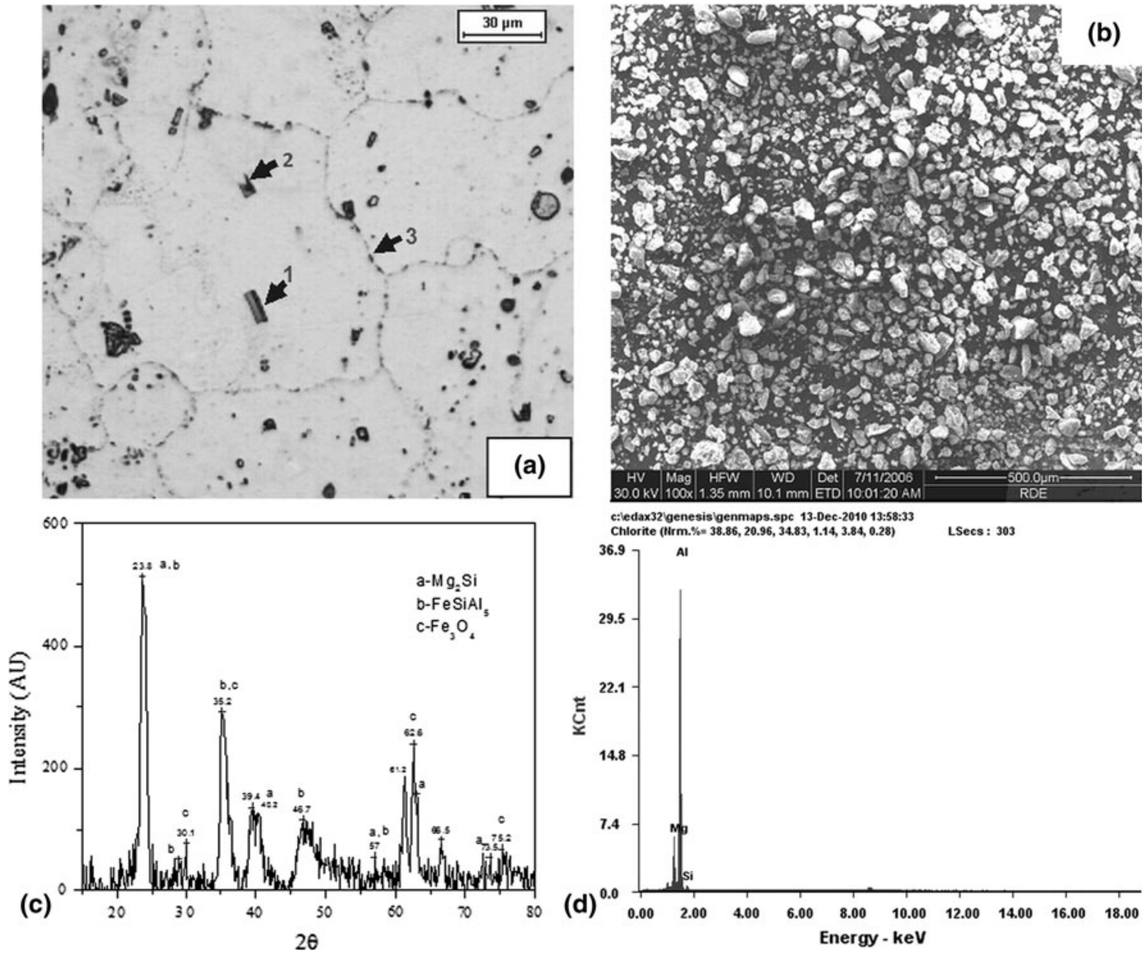

Fig. 1 (a) Optical image of Al-4Zn-2Mg alloy, (b) SEM image shows extracted particles from base alloy, (c) XRD pattern for the extracted particles, and (d) EDAX on Al with Mg_2Si particle

~10%. The UTS values for RRPA and RRNA showed 375 and 400 MPa, respectively. However, the ductility levels are reduced to 11 and 14%, respectively, compared to 21.5% for the CGPA sample (Fig. 4a).

The work hardening characteristics of the experimental alloy under different heat-treatment conditions was understood by plotting work hardening rate (θ), against flow stress ($\sigma - \sigma_y$) as shown in Fig. 4(b). It is well known that the work hardening characteristics of the aluminum alloy affect the yield strength and fracture toughness properties. Decreasing the work hardening temperature in case of cryorolled Al and Al-Mg alloy resulted in improved ductility without much loss in tensile strength (Ref 19). It was also shown that work hardening at lower temperature enables greater slip homogeneity and decreases the dynamic recrystallization effects. From the Fig. 4(b), it is evident that the work hardening behavior of cryorolled samples is superior to room temperature rolled samples. Apart from this, the alloy in naturally aged condition, showed better work hardening behavior as compared to that of artificially aged condition. The nature of work hardening is very much dependent on the dislocation storage mechanism rather than precipitate-dislocation interactions. Once the precipitates start forming, the work hardening behavior is dependent on precipitation hardening characteristics of the alloy. During artificial aging, large scale precipitation ensures that the dislocation storage mechanism is solely dependent on the nature, size, and distribution of precipitates rather than the grain size. This will result in higher yield strength in the case of artificially aged sample due to large scale precipitation and pinning the mobile dislocations that delays the yielding, which is also evident from the tensile curve of CRPA sample (Fig. 4a). However, in case of naturally aged sample, the yield strength was less as the number of precipitates available for pinning the dislocations, is less and thus dislocations become mobile at a lower applied strain.

Figure 5(a) and (b) shows TEM bright field images of the CRPA alloy, revealing fine precipitates evenly distributed within the matrix and absence of PFZ and a few grains of 100 nm in size. The average grain size measured from TEM images was 106 ± 25 nm. Figure 5(c) and (d) shows TEM bright field image of the RRPA and CRNA alloys, respectively. From Fig. 5(b) and (c), it is clear that the large number of sub-micron grains formed in case of CR than by room temperature rolling. Rolling at cryogenic temperature such as ~−170 °C, facilitated accommodation of large deformation due to suppression of dynamic recovery and absence of any annihilation of dislocations, resulting in fine grains as compared to room temperature rolling. The average grain size measured from TEM images in RRPA sample was 211 ± 45 nm. The TEM investigations also confirmed that the precipitates were more in the case of

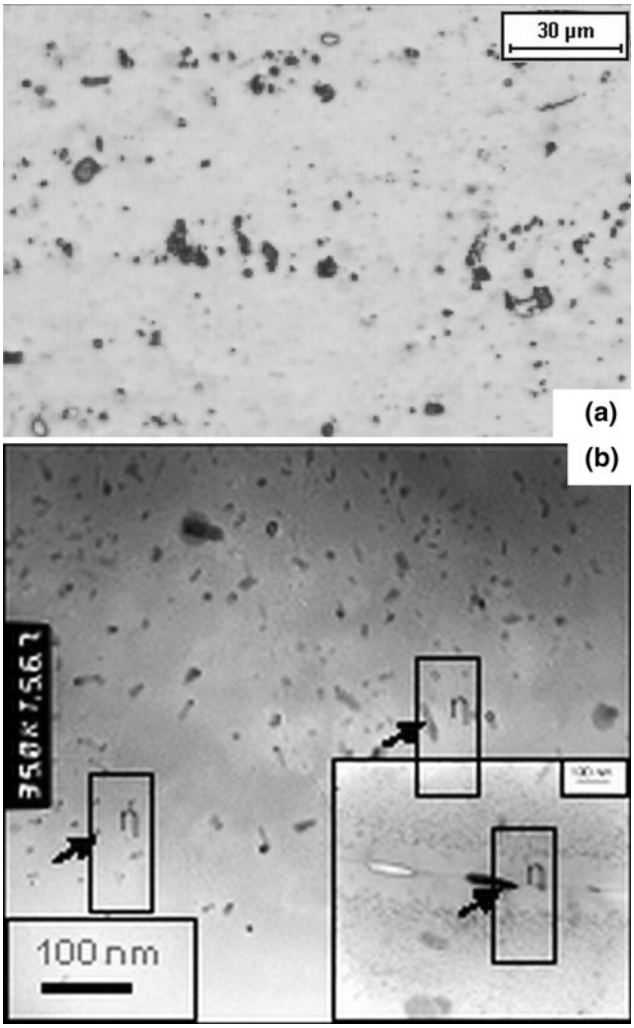

Fig. 2 (a) Light image of cryorolled sample, (b) TEM showing stable (η) and metastable (η′) precipitates, grain boundary precipitates (inset) and associated PFZ

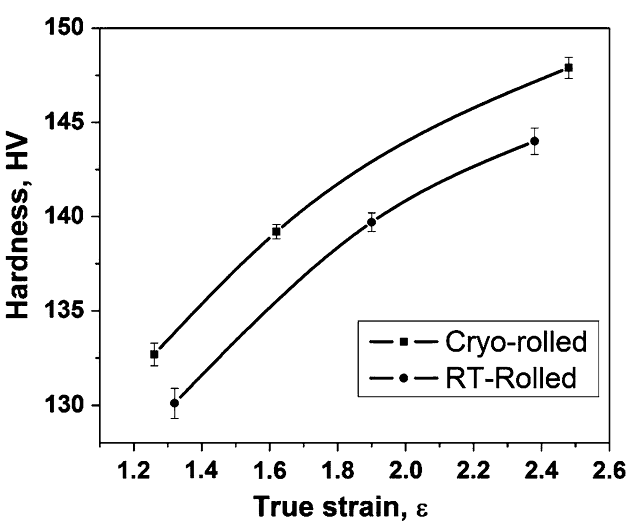

Fig. 3 True strain vs. hardness for cryo and room temperature rolled Al-4Mg-2Mg alloy

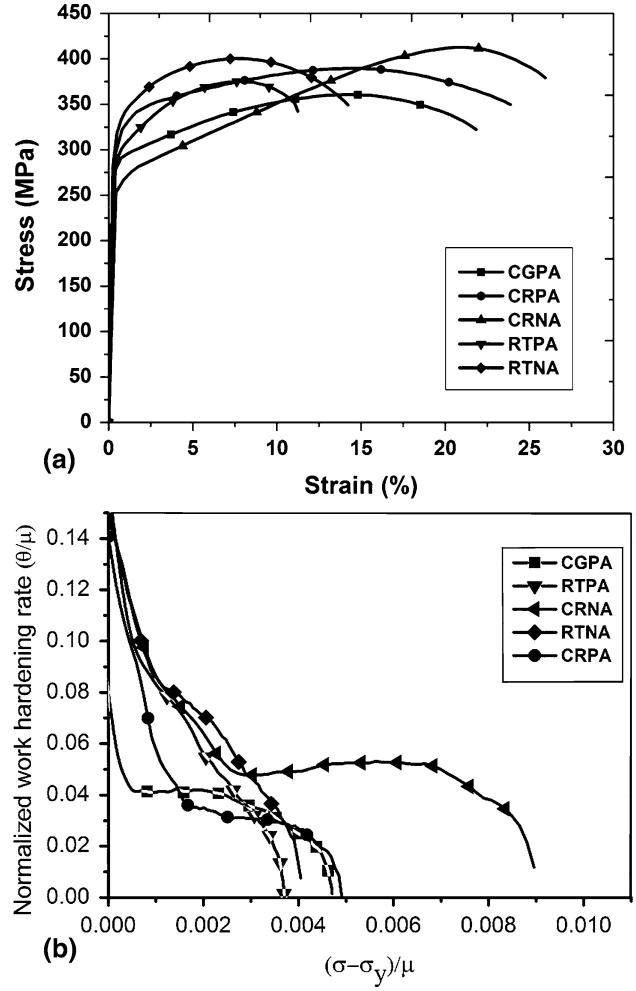

Fig. 4 (a) Engineering stress-strain curves for various treated Al-4Zn-2Mg alloys and (b) normalized work hardening rate curves corresponding to different processing and aging conditions

artificially aged condition than the naturally aged one. This is due to the fact that natural aging resulted in the formation of GP zones with only small volume fraction of η′ precipitate as shown in Fig. 5(d). It has already been reported that SPD process accelerates the formation of GP zones, but suppresses the nucleation and growth of the η′ phase in the T4 temper (Ref 20-23). The naturally aged material mostly contains shearable GP zones along with a high amount of solute, still in supersaturated state. In general, shearable precipitation does not allow additional dislocation storage and hence alloy should result in low-work hardening. However, in the present study, CRNA condition showed a continuous work hardening, until maximum strength. Hence, it can be interpreted that high amount of work hardening in CRNA condition, was due to dynamic precipitation, as reported earlier for the Al-Zn-Mg alloy (Ref 24). Dynamic precipitation is likely to occur by the growth of existing GP zones in this alloy. Again, this growth may occur by pipe diffusion along the dislocation line, during the waiting time of dislocations, at obstacles (Ref 24). High density of dislocations in cryorolled material acted as nucleation sites and increases formation of GP zones resulting in finer and more closely spaced GP zones. Subsequent deformation if any, (i.e., during tensile testing), the moving dislocations interact with

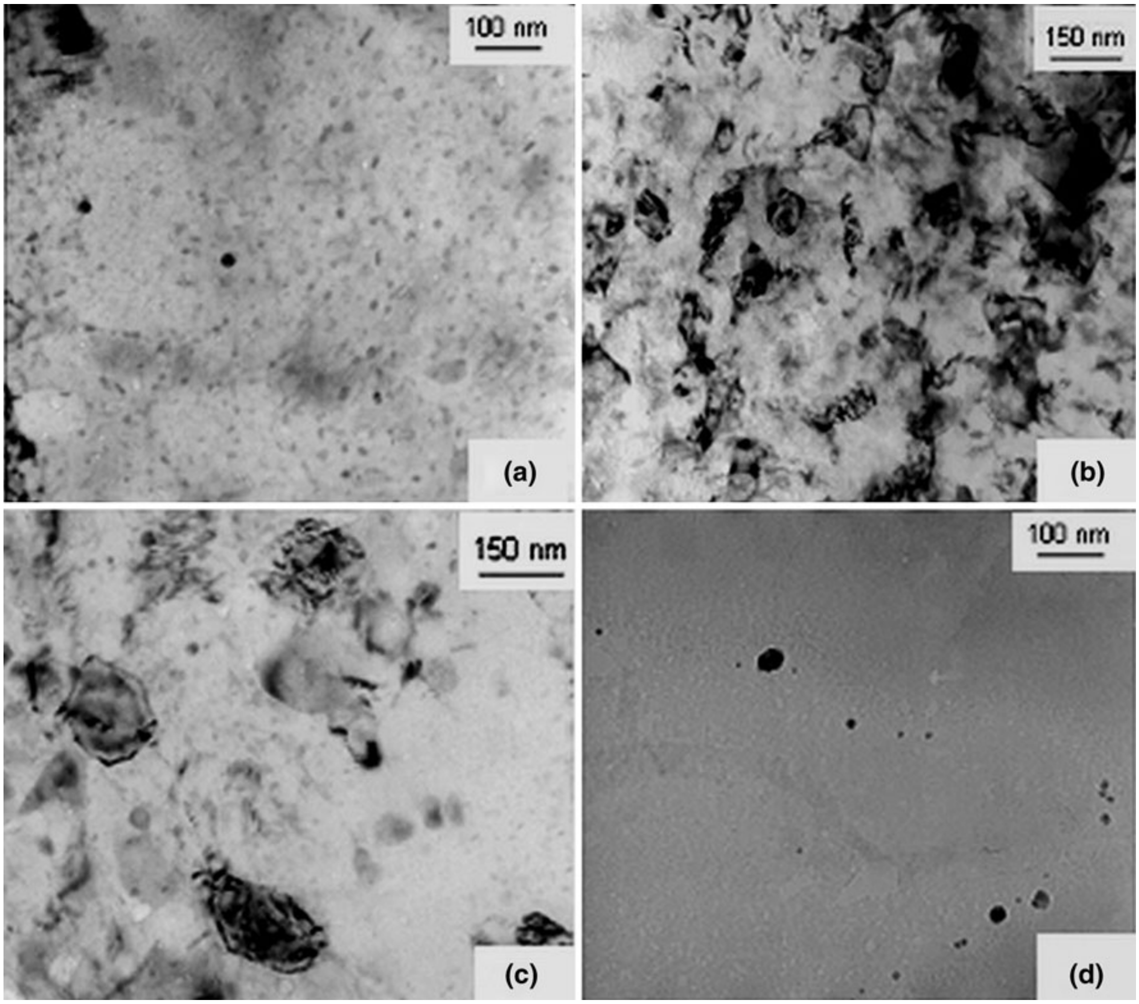

Fig. 5 TEM images of the alloy in different process conditions (a) and (b) CRPA, (c) RRPA, and (d) CRNA

solutes atoms in the matrix, leading to the formation and growth of precipitates. Therefore for CRNA, the amount of work hardening is high, as compared to CRPA condition.

In general, three microstructural changes occur during aging subsequent to rolling and short annealing:

(i) Grain growth during artificial aging, results in a decrease of the strength.
(ii) High density of dislocations generated during rolling mostly disappears due to recovery and recrystallization, resulting in decrease in strength and restoring ductility to some extent.
(iii) High density of G.P. zone and η′ precipitates, generated during aging, results in increased strength.

Hence, it is assumed that two opposing mechanisms are operative during aging subsequent to rolling and short annealing, i.e., (i) and (ii) promoting ductility and (iii) promoting strength. Net result of all these, should lead to an increased strength without compromising the ductility. It is evident from Fig. 3 that strength of cryorolled as well as room temperature rolled material is improved when compared to CGPA. This increase in strength could be attributed to smaller grain size, finer precipitates, and absence of PFZ. On rolling, dislocation density is increased that eventually act as nucleation sites for strengthening precipitates. This leads to finer precipitates in rolled alloys as compared to the CG alloy.

The strength of the sample is increased when its grain size is reduced. At the same time, by reducing the grain size to submicron level, slip distance is also reduced and hence the stress concentration lowers across the grain boundaries and grain boundary triple points. This resulted in improving the ductility levels (Ref 18, 25). Although rolling resulted in heavily deformed structure, further short annealing and aging resulted in a structure, having low-dislocation density with much scope for dislocation accumulation before saturation, which should increase the work hardening and hence improve ductility. Further improvement in ductility can be achieved through high density of fine precipitates, which provides effective sites for trapping and accumulation of dislocations.

Higher level of dislocation density can be uniformly stored in the material rolled at cryogenic temperatures as a result of the suppressed annihilation of dislocations, which if present, should occur at grain boundary and in the lattice through thermally activated cross-slip and climb. Hence, ductility of room temperature rolled material was found to be much lower, compared to cryorolled samples, which was comparable to that of coarse-grained material.

Hence, it can be concluded from the observation that for simultaneously achieving increased strength as well as good ductility, the microstructure should have high density of finer second-phase precipitates and adequate dislocation density. In the present study it is demonstrated, that simultaneous improvement in strength as well as ductility can be achieved in the base Al-4Zn-2Mg alloy, through CR and heat-treatment combinations.

4. Conclusions

The aging and tensile behavior of an Al-4Zn-2Mg alloy subjected to RT and CR was investigated. Following conclusions are drawn from the results.

Peak aging, after CR and short annealing showed an increased strength while retaining ductility as compared to CGPA. However, peak aging after RT rolling resulted in increased strength with loss in ductility, as compared to CGPA. An improved strength and ductility of Al-4Zn-2Mg alloys, subjected to CR, is attributed mainly due to ultrafine-grain structure combined with controlled aging, resulting in finer precipitates and presence of dislocations. High amount of work hardening behavior for CRNA is attributed to dynamic precipitation during tensile deformation. The results also demonstrated, a successful method for increasing the strength while retaining the ductility, with respect to heat treatable Al-4Zn-2Mg alloy, by employing CR.

Acknowledgments

The authors are grateful to Dr. S. Srikanth, Director, National Metallurgical Laboratory, Jamshedpur, India for his encouragement and extending the necessary support for the work.

References

1. Z.Y. Liu, G.X. Liang, E.D. Wang, and Z.R. Wang, The Effect of Cumulative Large Plastic Strain on the Structure and Properties of a Cu-Zn Alloy, *Mater. Sci. Eng. A*, 1998, **242**, p 137–140
2. B. Mingler, H.P. Karnthaler, M. Zehetbauer, and R.Z. Valiev, TEM Investigation of Multidirectionally Deformed Copper, *Mater. Sci. Eng. A*, 2001, **319–321**, p 242–245
3. C. Xu, M. Furukawa, Z. Horita, and T.G. Langdon, Severe Plastic Deformation as a Processing Tool to Develop Superplastic Metals, *J. Alloys Compd.*, 2004, **378**, p 27–34
4. Z. Horita, T. Fujinami, M. Nemoto, and T.G. Langdon, Equal Channel Angular Pressing of Commercial Aluminum Alloys: Grain Refinement Thermal Stability and Tensile Properties, *Metall. Mater. Trans.*, 2000, **A31**, p 691–701
5. S.J. Oh and S.B. Kang, Analysis of the Billet Deformation During Equal Channel Angular Pressing, *Mater. Sci. Eng.*, 2003, **A343**, p 107–115
6. Y.Y. Wang, P.L. Sun, P.W. Kao, and C.P. Chang, Effect of Deformation Temperature on the Microstructure Developed in Commercial Purity Aluminum Processed by Equal Channel Angular Extrusion, *Scr. Mater.*, 2004, **50**, p 613–617
7. Y. Saito, H. Utsunomiya, N. Tsuji, and T. Sakai, Novel ultra-High Straining Process for Bulk Materials Development of the Accumulative Roll-Bonding (ARB) Process, *Acta Mater.*, 1999, **47**, p 579–583
8. N. Tsuji, Y. Siato, H. Utsunomiya, and S. Tanigawa, Ultra-Fine Grained Bulk Steel Produced by Accumulative Roll-Bonding (ARB) Process, *Scr. Mater.*, 1999, **40**, p 795–800
9. S.H. Lee, Y. Saito, H. Utsunomiya, N. Tsuji, and T. Sakai, Role of Shear Strain in Ultra Grain Refinement by Accumulative Roll-Bonding (ARB) Process, *Scr. Mater.*, 2002, **46**, p 281–285
10. K.T. Park, H.J. Kwon, W.J. Kim, and Y.S. Kim, Microstructural Characteristics and Thermal Stability of Ultrafine Grained 6061 Al Alloy Fabricated by Accumulative Roll Bonding Process, *Mater. Sci. Eng.*, 2001, **A316**, p 145–152
11. J.Y. Huang, Y.T. Zhu, H. Jiang, and T.C. Lowe, Microstructures and Dislocation Configurations in Nanostructured Cu Processed by Repetitive Corrugation and Straightening, *Acta Mater.*, 2001, **49**, p 1497–1505
12. J.Y. Huang, Y.T. Zhu, J. David, and T.C. Lowe, Development of Repetitive Corrugation and Straightening, *Mater. Sci. Eng.*, 2004, **A371**, p 35–39
13. Y.T. Zhu, H. Jiang, J.Y. Huang, and T.C. Lowe, A New Route to Bulk Nanostructured Metals, *Metall. Mater. Trans.*, 2001, **A32**, p 1559–1562
14. D.H. Shin, J.J. Park, Y.S. Kim, and K.T. Park, Constrained Groove Pressing and Its Application to Grain Refinement of Aluminum, *Mater. Sci. Eng.*, 2002, **A328**, p 98–103
15. J.W. Lee and J.J. Park, Numerical and Experimental Investigations of Constrained Groove Pressing and Rolling for Grain Refinement, *Mater. Process. Technol.*, 2002, **130**, p 208–213
16. Y.B. Lee, D.H. Shin, K.T. Park, and W.J. Nam, Effect of Annealing Temperature on Microstructures and Mechanical Properties of a 5083 Al Alloy Deformed at Cryogenic Temperature, *Scr. Mater.*, 2004, **51**, p 355–359
17. T. Shanmugasundaram, B.S. Murty, and V. Subramanya Sarma, Development of Ultrafine Grained High Strength Al-Cu Alloy by Cryorolling, *Scr. Mater.*, 2006, **54**, p 2013–2017
18. S. Cheng, Y.H. Zhao, Y.T. Zhu, and E. Ma, Optimizing the Strength and Ductility of Fine Structured 2024 Al Alloy by Nano-Precipitation, *Acta Mater.*, 2007, **55**, p 5822–5832
19. D. Chu and J.W. Morris, *Influence of Grain Structure and Solute Composition on the Work Hardening Behavior of Aluminium at Cryogenic Temperatures,* LBL 34019 Lawrence Berkeley Laboratory and University of California
20. P.N. Adler, R. Delasi, and G. Geschwind, Influence of Microstructure on the Mechanical Properties and Stress Corrosion Susceptibility of 7075 Aluminum Alloy, *Metall. Trans.*, 1972, **A3**, p 3191–3200
21. J.T. Staley, Aging Kinetics of Aluminum Alloy 7050, *Metal. Trans.*, 1974, **A5**, p 929–932
22. O.B. Lung, Y. Ji-Gang, and Y. Chen-Kuo, Effects of Step-Quench and Aging on Mechanical Properties and Resistance to Stress Corrosion Cracking of 7050 Aluminum Alloy, *Mater. Trans. JIM*, 2000, **41**, p 783–789
23. Y.H. Zhao, X.Z. Zhao, X.Z. Liao, Z. Jin, R.Z. Valiev, and Y.T. Zhu, Microstructures and Mechanical Properties of Ultrafine Grained 7075 Al Alloy Processed by ECAP and Their Evolutions During Annealing, *Acta Mater.*, 2004, **52**, p 4589–4599
24. A. Deschamps, M. Niewczas, F. Bley, Y. Brechet, D. Embury, L. Lesinq, and F. Livet, Low Temperature Dynamic Precipitation in a Supersaturated Al-Zn-Mg Alloy and Related Strain Hardening, *Philos. Mag.*, 1999, **A79**, p 2485–2504
25. L.J. Zheng, C.Q. Chen, T.T. Zhou, P.Y. Liu, and M.G. Zeng, Structure and Properties of Ultrafine-Grained Al-Zn-Mg-Cu and Al-Cu-Mg-Mn Alloys Fabricated by ECA Pressing Combined With Thermal Treatment, *Mater. Charact.*, 2002, **49**, p 455–461